2017

Palynostratigraphy and Environmental Implication of Organic-walled Microfossils Recovered from IODP Site U1435

Mitchell Clifford Gregory
Louisiana State University and Agricultural and Mechanical College

PALYNOSTRATIGRAPHY AND ENVIRONMENTAL IMPLICATION OF ORGANIC-WALLED MICROFOSSILS RECOVERED FROM IODP SITE U1435

A Thesis

Submitted to the Graduate Faculty of the
Louisiana State University and
Agricultural and Mechanical College
in partial fulfillment of the
requirements for the degree of
Master of Science

in

The Department of Geology and Geophysics

by
Mitchell Clifford Gregory
B.S., Louisiana State University, 2014
August 2017

ACKNOWLEDGMENTS

This research used samples and/or data provided by the International Ocean Discovery Program (IODP). Funding for this research was provided by U.S. Science Support Program to Louisiana State University. The research was carried out at the Center for Excellence in Palynology (CENEX) in Baton Rouge, Louisiana.

I would like to acknowledge and thank my advisor Dr. Sophie Warny for all of her tremendous support and guidance during my research. I would like to thank my committee members, Dr. Peter Clift and Dr. Carol Wilson, for their useful feedback and constructive criticisms of this work. Thank you to Dr. Gilles Escarguel for his help with the statistical analyses presented here, to Dr. Yunfa Miao for sharing his knowledge of Asian palynomorphs, and to Chang Liu for his help with understanding the history of the South China Sea. I would like to thank the other students who have worked in the CENEX lab group for both their technical and moral support during this process, as well as all those in the Geology and Geophysics Department at LSU who have made my time as a graduate student an enjoyable one. Finally, I must thank my family and friends who have always been there for me, especially through the challenges of being a graduate student.

TABLE OF CONTENTS

ABSTRACT

Extensive studies have examined the syn- and post-rift sediments in the South China Sea and surrounding margins, but pre-rift, Eocene deposits are rare. Here we examine organic-walled microfossils from the South China Sea, recovered at Site U1435 of IODP Expedition 349 to provide palynostratigraphic control and characterize the environmental setting before, and in response to, the initiation of seafloor spreading in the basin ~33 Ma. The well preserved palynological assemblage recovered allow dating of sediments sampled at Site U1435. Units II and III are now subdivided in 4 subzones; Zone 1 is essentially barren, Zones 2 and 3A are assigned an age of 50.5 to 40.6 Ma, Zone 3B likely ranges from 40.6 to 33.9 Ma (Unit II is thus Eocene in age), and Zone 4 (Unit IB) is likely ranging from 33.9 to 30.72 Ma (early Oligocene in age). The lack of palynomorphs and the extreme thermal maturity of the palynomorphs recovered in Zone 1 is believed to be associated to intense volcanism in proximity to site U1435. A decrease in terrestrial palynomorphs and the first appearance of *Homotryblium plectilum* at 40.6 Ma, both indicative of sea level rise, permits the integration of our biostratigraphic data into a sequence stratigraphic framework. This event is believed to be associated with the TA3.5 sequence cycle highstand in the lower Bartonian with the TA3.5 maximum flooding surface (41.2 Ma) marking the Lutetian/Bartonian boundary (middle Eocene).

The palynological assemblage also provided valuable information on the environmental evolution in the northern South China Sea. The Eocene time interval sampled is characterized by abundant spores and *Homotryblium* spp. dinoflagellates, both indicative of a nearshore setting, with abundant palms and *Spinizonocolpites* spp. mangroves characteristic of a warm everwet environment. The lower Oligocene is characterized by decreasing abundance in spores, palms, and mangroves along with increasing conifers, thus indicating that the early Oligocene cooling

was felt in the South China Sea as well. An acme of a new dinoflagellate, referred to herein as *Spiniferites* cf. *pseudofurcatus* is a new marker of the Eocene/Oligocene boundary, of potential regional value as characteristic of the newly opening South China Sea.

1. INTRODUCTION

The South China Sea is a marginal sea, which formed at the junction of the Eurasian, Indo-Australian, and Pacific plates (Fig. 1). The South China Sea covers a total area of about 3.5 x 10^6 km^2 and is bordered by China to the north, Malaysia to the south, the Philippines to the east, and Vietnam to the west. Despite extensive studies of the area, the complex geologic history of the South China Sea remains unclear.

IODP Expedition 349 set out to further study the tectonic and climatic history of the South China Sea by sampling into igneous basement rock in the deep basin and the overlying sedimentary deposits. The expedition drilled five sites throughout the South China Sea to better constrain the initial timing of the opening and evolution of seafloor spreading of the basin, and to examine paleoceanographic and sedimentary responses to its formation. This study focused on samples from Site U1435, which is located on the continental side of the continent/ocean boundary characterized with a topographic high elevation.

Drilling at Site U1435 (Fig. 2) recovered a 300.0 m cored section, which is divided into three lithostratigraphic units based on on-board macroscopic and microscopic description. Unit I was assigned an Oligocene to Pleistocene based on nannofossil and planktonic foraminifer recovery age while Unit II and Unit III were referred to as of an uncertain pre-Oligocene age (Fig. 3) because of the lack or poor preservation of nannofossil and foraminifer markers in these lower sections. Unit I and Unit II are separated by a hiatus interpreted as the breakup unconformity associated with the onset of seafloor spreading in the South China Sea (Expedition 349 Scientists 2014; Li et al. 2016).

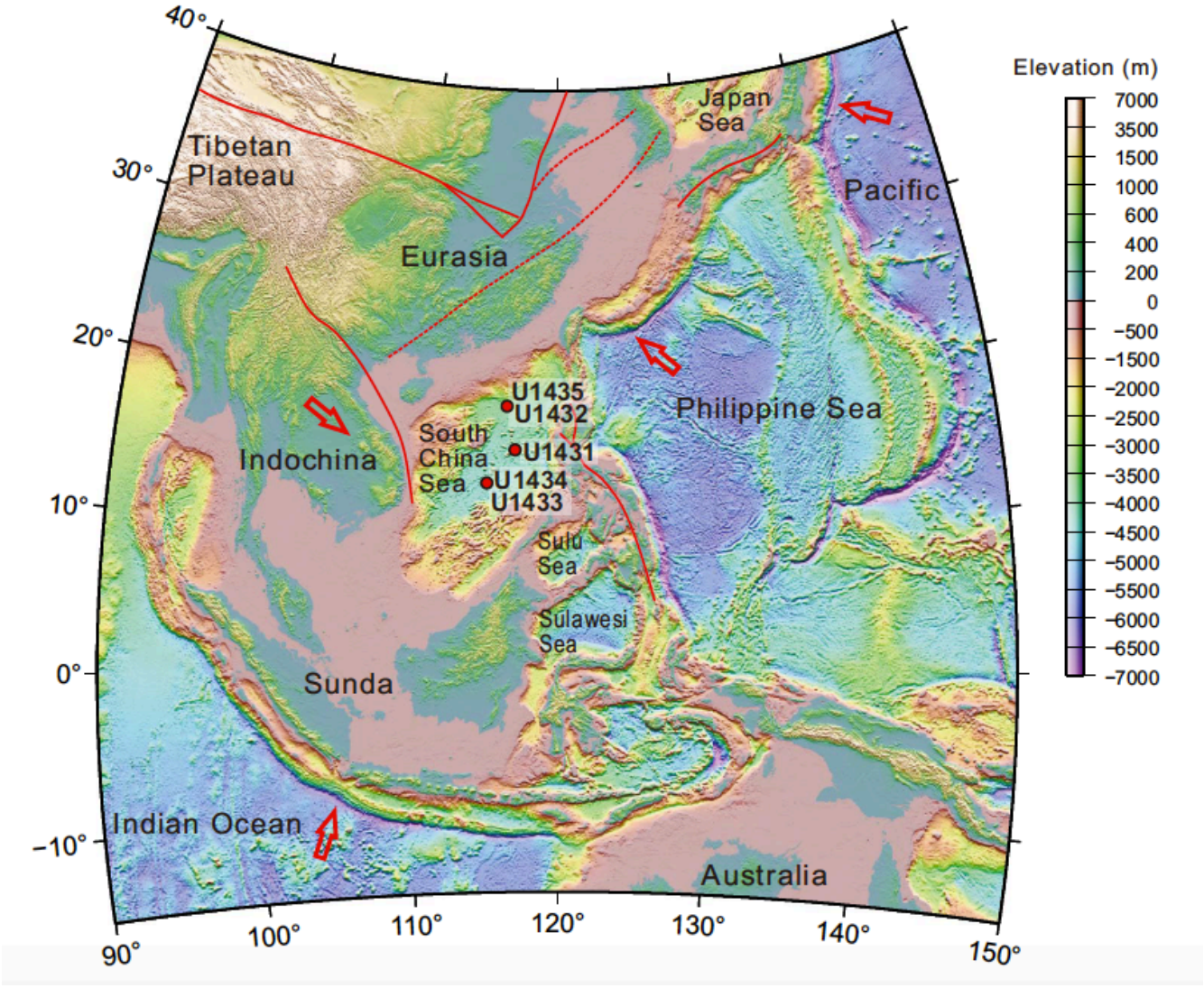

Figure 1. Regional topographic map and tectonic framework. Red lines = regional faults. Red arrows indicate direction of plate movement (Li et al. 2015).

In this study, we present a palynological analysis of Site U1435 to provide age control for the pre-breakup sediments (Unit II and Unit III) and characterize the paleoenvironmental response to the rifting and eventual seafloor spreading of the South China Sea in the Paleogene.

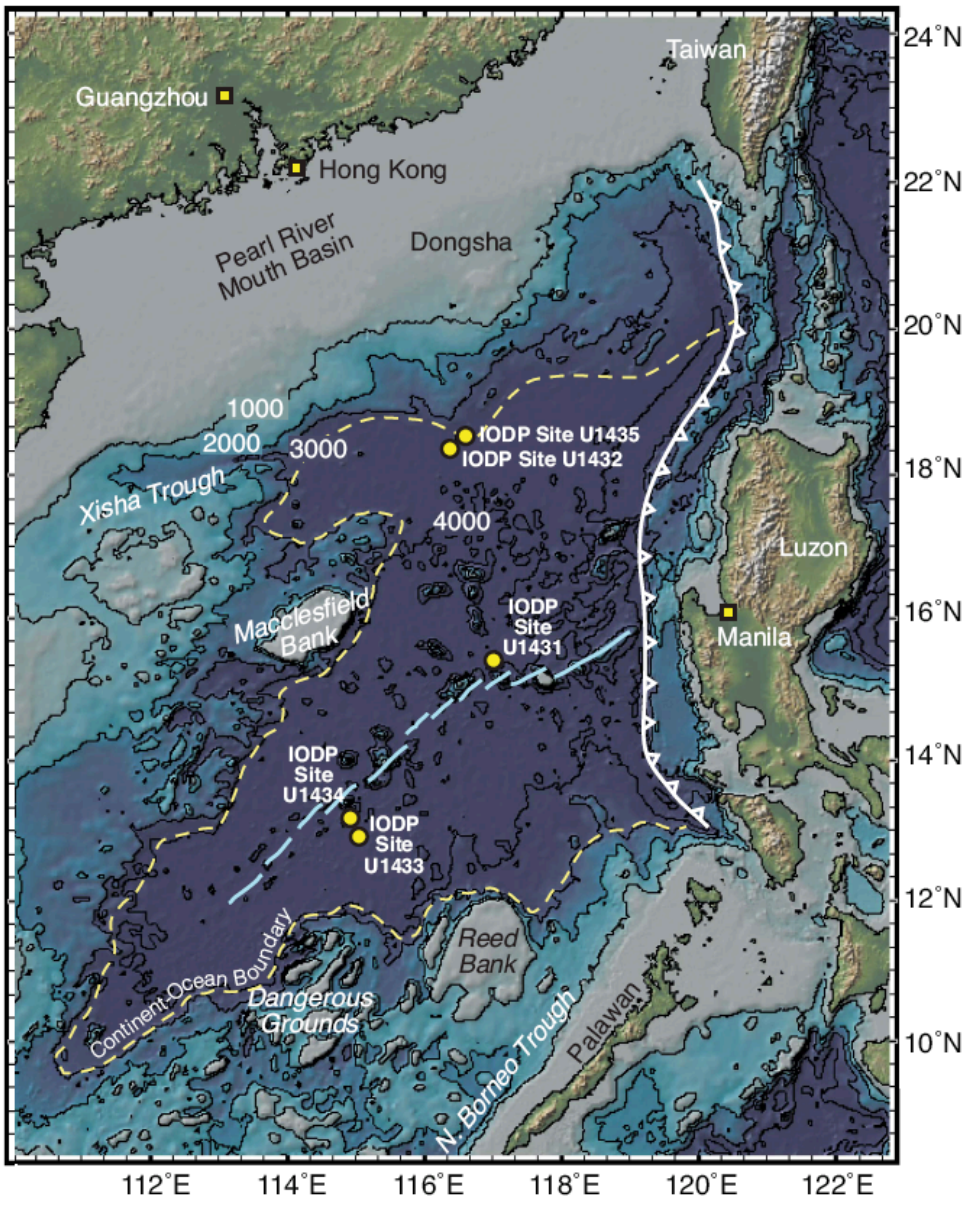

Figure 2. Figure 1. Bathymetric map of the South China Sea with IODP Expedition 349 drilling sites. Yellow dashed line = continent/ocean boundary, blue lines = relict South China Sea spreading center, white line with triangles = Manila Trench (Li et al. 2015).

2. GEOLOGIC SETTING

Tectonic events in the South China Sea area can be traced back through the Mesozoic. Subduction of the paleo-Pacific plate beneath the Eurasian plate took place during the Mesozoic along what is now the northeastern continental margin of the South China Sea (Jahn et al. 1976; Holloway 1982; Taylor and Hayes 1983; Hayes et al. 1995; Zhou and Li 2000). This subduction emplaced igneous rocks and led to the formation of a wide orogenic belt in Southeast Asia (Zhou and Li 2000*).* Regional extension is believed to have begun in the Late Cretaceous, which led to continental margin rifting and eventually seafloor spreading in the Cenozoic ~32 Ma (Taylor and Hayes 1980, 1983). Drilling results from IODP Expedition 349 led to a refinement of the initial spreading age to ~33 Ma (Li et al., 2014). The opening mechanism for the South China Sea is still however the source of debate (Tapponnier et al. 1982; Taylor and Hayes 1980, 1983; Holloway 1982; Briais et al. 1993; Leloup et al. 2001; Flower et al. 2001; Hall 2002; Xu et al. 2012).

3. MATERIALS AND METHODS

IODP Expedition 349 was conducted aboard the Joint Oceanographic Institutions for Deep Earth Drilling (*JOIDES*) *Resolution* scientific drilling ship. Site U1435 samples were collected using a rotary core barrel (RCB) coring system. The RCB cored to a depth of 300.0 mbsf and obtained 171.37 m of sediment with a recovery rate of 57.1% (Li et al. 2015).

IODP Site U1435 is located at 18° 33.3466 N, 116° 36.6174 E in a water depth of 3252.5 meters (Fig. 2).Based on the lithology description combined with other measurements, the Shipboard Scientific Party defined three lithostratigraphic units within the cored section (Expedition 349 Scientists 2014). The lowermost unit, Unit III (275.54 – 300.00 mbsf) contains dark gray silty sandstone, silty mudstone, and minor conglomerate, and this unit is considered to be a finer-grained unit than the overlying Unit II. Unit II (77.65 – 275.54 mbsf) represents the majority of the cored section and is composed of an averagely medium-grained dark gray silty sandstone. The uppermost Unit I (0 – 77.65 mbsf) is subdivided into two subunits as Unit IA (0 – 36.04 mbsf) and Unit IB (36.04 – 77.65 mbsf). Unit IB is mostly greenish gray nannofossil-rich clay and some greenish gray clay. Samples from Unit IA are not analyzed in this study.

A total of 46 samples were collected for palynological analysis. Figure 4 displays the depth where the samples were collected. Samples were sent to Global Geolab Limited for processing. Samples were weighed and spiked with *Lycopodium* tablets containing a known quantity of exotic *Lycopodium* spores to use for palynomorph concentration calculations. Carbonates were digested from the samples using 10% HCl, and silicates were digested using 70% HF. Palynomorphs were then separated by placing the residue in $ZnBr_2$ (density = 2.00g/mL), a heavy liquid, allowing them to float above the mineral fraction contained in the

residue. The samples were sieved through a 10 μm filter and mounted in glycerine jelly on glass slides for analysis (Brown 2008).

Samples were analyzed using an Olympus BX41 light microscope at 60x magnification. A QCapture camera attached to the microscope was used to take photomicrographs of palynomorphs using QCapture software. At least 300 palynomorphs were identified and counted per sample, when possible. After identification and tabulation of palynomorphs, concentrations were calculated based on *Lycopodium* recovery for each sample. The counted *Lycopodium* spores relative to the known amount of spores added before processing was used to estimate palynomorph recovery and the amount present in each sample before processing, following the

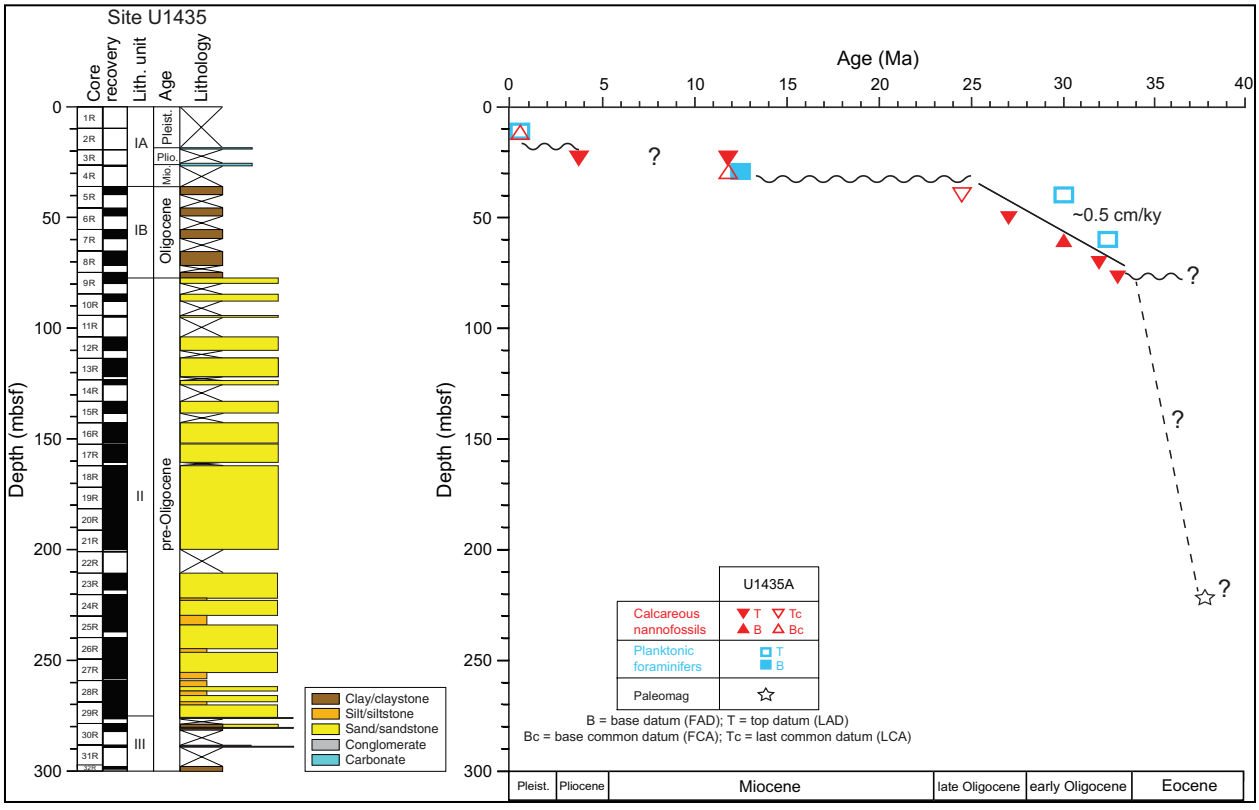

Figure 3. IODP Expedition 349 Shipboard age-depth model based on calcareous nannofossils and benthic foraminifers. FAD = first appearance datum, LAD = last appearance datum, FCA = first common appearance, LCA = last common appearance. Wavy line = possible hiatus (Li et al. 2015).

equation of Benninghoff (1962). $C=(Pc\times Lt\times T)/(Lc\times W)$, where C = concentration (specimens per gram of dried weight of sediment sampled, or gdw^{-1}), Pc = the number of palynomorphs counted, Lt = the number of *Lycopodium* spores per tablet, T = the total number of *Lycopodium* tablets added per sample, Lc = the number of *Lycopodium* spores counted in the sample, and W = the weight of dried sediment (with dried weight (dw) in grams).

4. PALYNOLOGICAL RESULTS, STATISTICAL ANALYSIS, AND PROPOSED PALYNOLOGICAL ZONATIONS

Of the 46 samples analyzed, the upper 23 samples (5R 1W to 14R 1W) are palynologically productive with counts of at least 300 palynomorphs. Samples 15R 2W and 16R 3W do not reach 300 palynomorphs, but at least 100 palynomorphs are counted, and these samples are included in the analyses. The lowermost 21 samples (17R 1W to 32R 1W) do not produce statistically significant counts of at least 100 palynomorphs, thus they are excluded from the statistical analyses.

The palynomorph assemblage is divided here into 12 separate groups based on abundance or morphological/ecological similarities (Fig. 4). Dinoflagellate cysts are divided into 5 groups: *Cordosphaeridium* spp. (including *C. fibrospinosum*), *Homotryblium* spp. (including *H. plectilum* and *H. tenuispinosum*), *Spiniferites* spp. (mostly *S. ramosus*), *Spiniferites* cf. *pseudofurcatus*, and "Other Dinocysts," which groups all other dinoflagellate cysts and acritarchs. A diverse assemblage of over 100 morphologically distinct pollen and spores is observed in the samples, but the terrestrial palynomorphs are divided here into 7 groups: "Spores" (all monolete and trilete spores), Taxodiaceae (including fossil types), bisaccate pollen, Gramineae (including fossil types), palms (monocolpate/monosulcate forms and *Dicolpopollis* spp.), the mangrove pollen *Spinizonocolpites* spp. (including extant *Nypa* type), and all other angiosperm types (mostly tricolpate and tricolporate forms). Common palynomorphs are depicted in Plate 1 and Plate 2.

4.1. Statistical analysis

Multivariate analyses and significance tests were performed on the palynologically productive samples (5R 1W to 16R 3W) and are described by 12 variables (the 12 palynomorph

groups). All analyses are based on a Bray-Curtis similarity matrix, using PAST v. 3.15 (available at https://folk.uio.no/ohammer/past/).

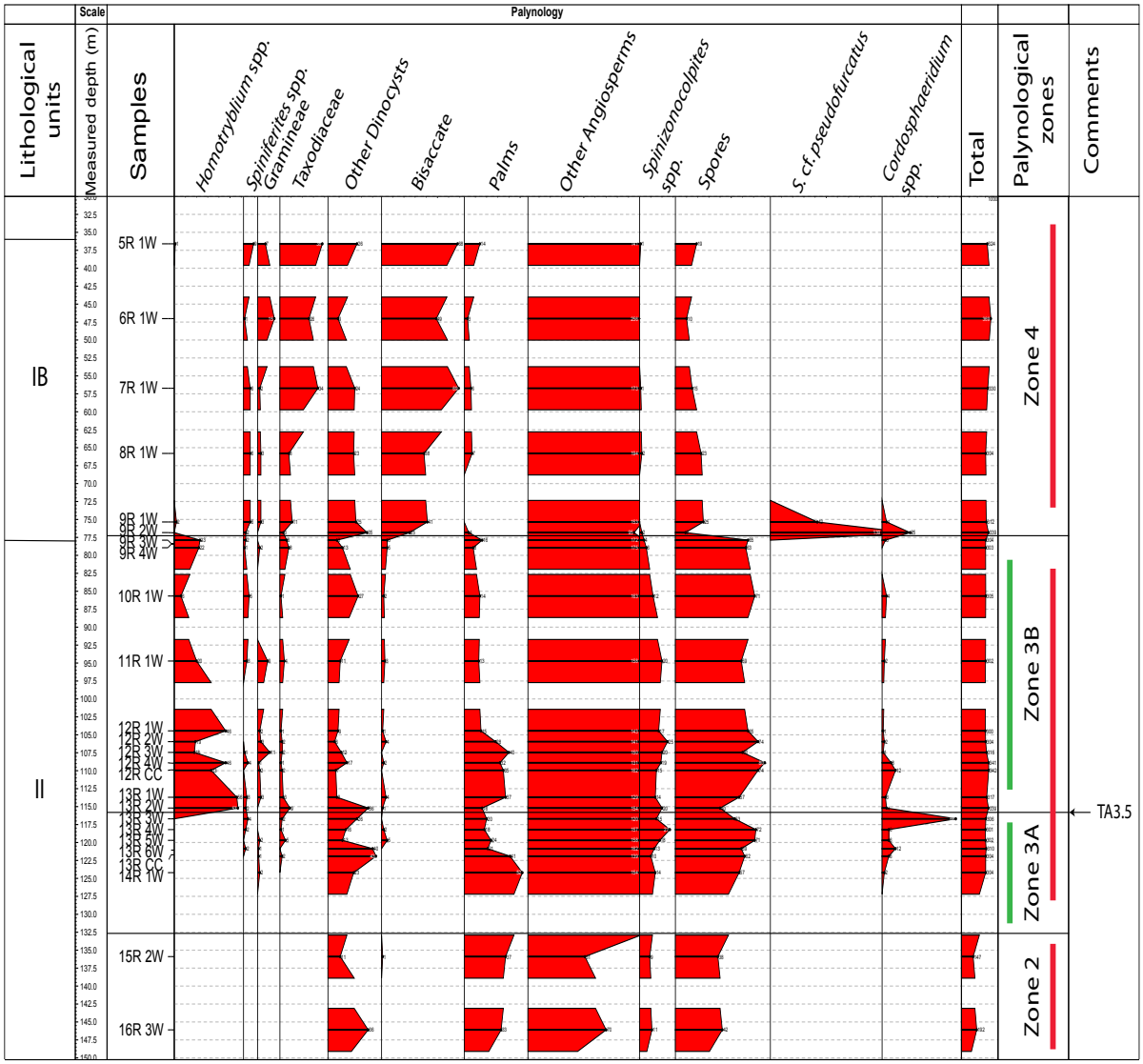

Figure 4. Palynomorph group assemblage of Site U1435 plotted as raw point counts in order of first down-hole occurrence. Red bars indicate three major clusters from hierarchical Cluster Analysis (hCA). Green bars indicate sub-clusters of second major cluster from hCA (see Figure 5 for details). Lithological unit divisions based on Expedition 349 Scientists (2014).

A hierarchical Cluster Analysis (hCA) using the stratigraphically-constrained UPGMA clustering algorithm was performed to identify clusters that follow the stratigraphic order of samples (Fig. 5). This analysis clearly defines three groups within these samples (red boxes),

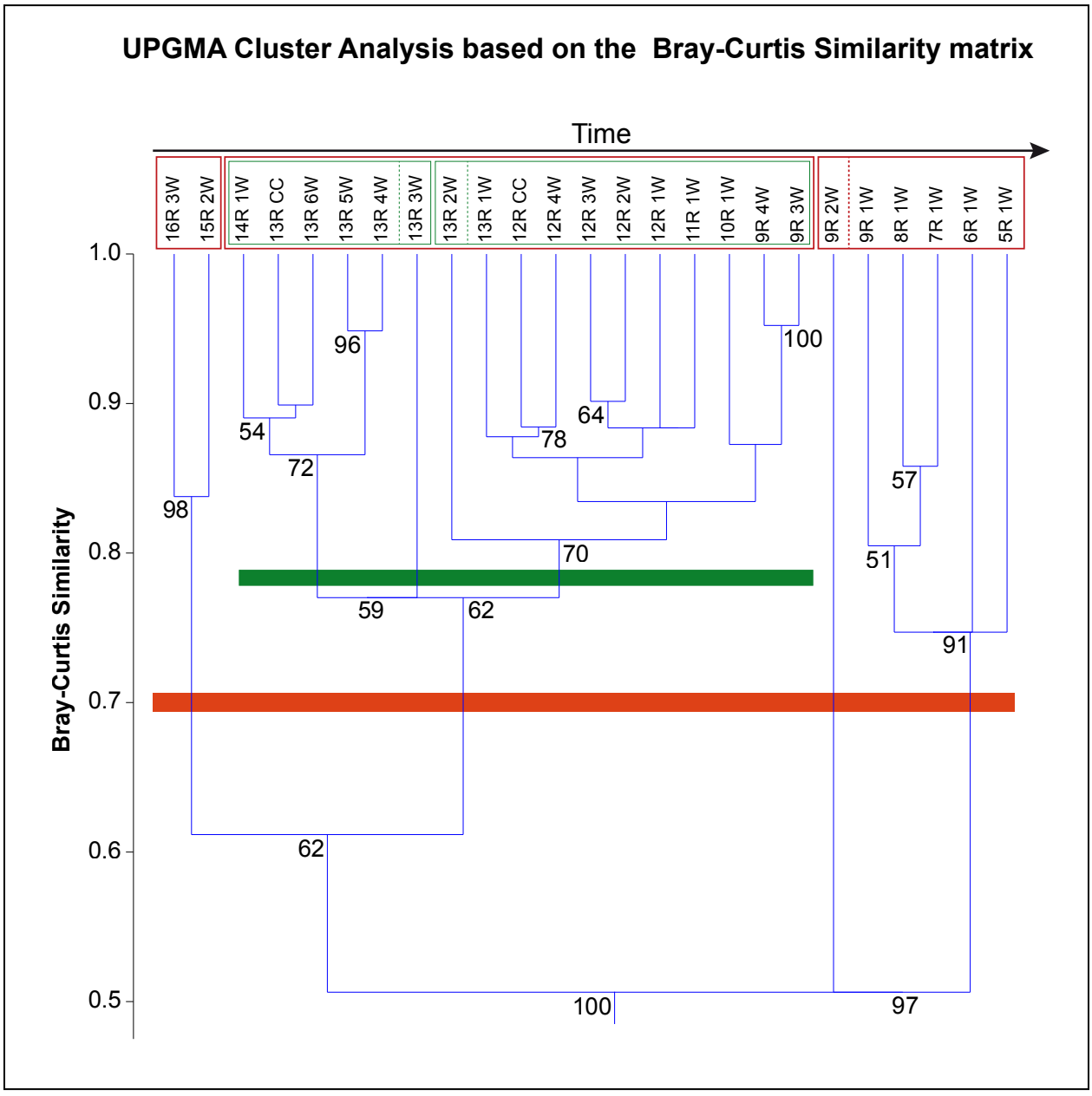

Figure 5. Hierarchical Cluster Analysis based on the 12 palynomorph groups described, and from samples with statistically significant palynomorph recovery.

with the second group (14R 1W to 9R 3W) further subdivided into two sub-clusters (green boxes). The three red clusters are separated at a Bray-Curtis similarity value of ~0.70 (red line, Fig. 5), and the two green sub-clusters are separated at a Bray-Curtis similarity value of ~0.80 (green line, Fig. 5). Bray-Curtis similarity values range between 0 and 1, with values closer to 1

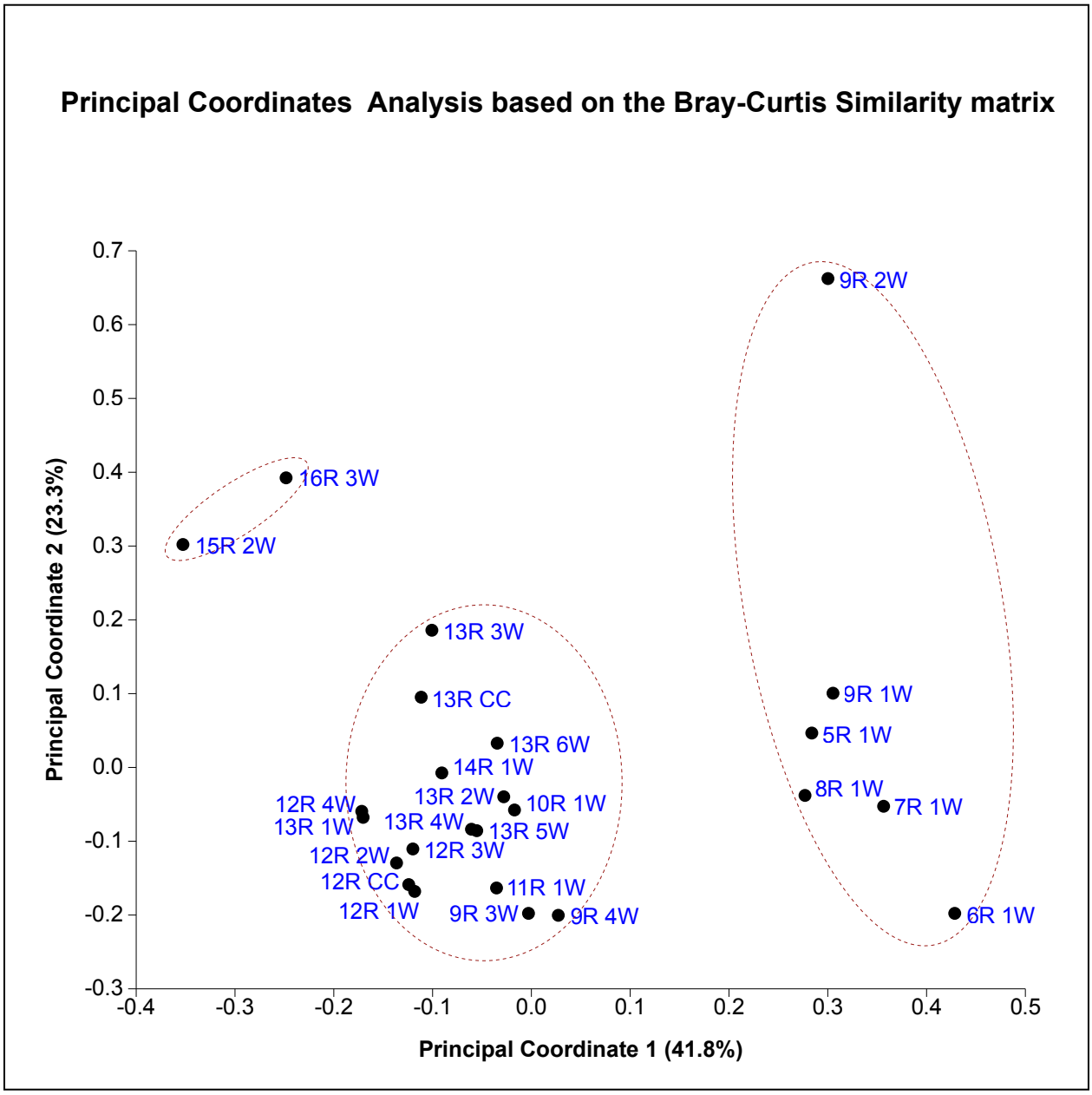

Figure 6. Principal Coordinates Analysis of the two first Principal Coordinates (PCo1 vs. PCo2).

indicating clusters that are more similar. Samples within dashed lines (13R 3W, 13R 2W, 9R 2W) are considered transitional in composition between the adjacent clusters or sub-clusters. Bootstrap support values, estimated through 1000 bootstrap replicates, are noted at the hCA tree nodes. These values range from 0 to 100% and indicate the statistical confidence level for the corresponding cluster (values below 50% suggest unsupported clusters and are not indicated).

Results of the Principal Coordinate Analysis (PCoA) are illustrated in Figure 6 and Figure 7 and focus on multivariate gradients within the data. Within the statistically significant dataset, the two first Principal Coordinates capture 65.1% of the overall multivariate variability (Fig. 6). Here, the three main clusters (red-dashed circles) identified in the hCA are also clearly separated and ordered correctly along the first Principal Component. This ordering is also evident when the first Principal Component is plotted against depth (Fig. 7). The first Principal Component captures the main source of inter-sample variability along the "Depth" axis as 79% of the variation within the first Principal Component is explained by sample's depth. The sub-clusters identified in Figure 5 (green boxes) also show a trend in increasing first Principal Component value (green dashed arrows).

Two one-way Analysis of Similarity tests (ANOSIM) were then performed using the same Bray-Curtis similarity matrix (Fig. 8). The ANOSIM test is a non-parametric significance test contrasting within-group and between-group inter-sample similarities. If the sample clusters seen in Figures 5 to 7 are "real" (i.e., if samples within a given cluster show randomly different relative abundances of the 12 original descriptors, and samples from different clusters show non-randomly different relative abundances of the 12 descriptors), the average similarity between samples from a given cluster should be higher than the average similarity between samples from two or more different clusters. A low p-value (<0.05) indicates that the null hypothesis of

ANOSIM (that clusters randomly differ from each other) can be rejected since the compared clusters non-randomly differ from each other.

A three-group ANOSIM test of the three main clusters (red boxes in Fig. 5) indicates that the three clusters highly significantly differ from each other ($p < 0.00001$). These clusters also significantly differ at the pair-wise level (cluster 1 vs. cluster 2: $p = 0.0059$; cluster 2 vs. cluster 3: $p = 0.00003$). A two-group ANOSIM test shows that the two sub-clusters (green boxes in Fig. 5) within cluster 2 significantly differ from each other, as well ($p = 0.0027$). The ANOSIM tests confirm that the four clusters identified from the hCA (Fig. 5) non-randomly differ from each other based on the 12 original descriptors.

Following the results of the ANOSIM tests, a SIMPER analysis (Fig. 8) was performed to identify the descriptors driving the among-group differences. Results from the SIMPER analysis aid in the interpretations of paleoenvironmental changes between the deposition of the clustered samples. The SIMPER analysis results focus on which one of the palynomorph groups are contributing to the changes between clusters or sub-clusters. Based on the SIMPER analysis results, 4 of the 12 original descriptors are identified as playing a major role in differentiating the clusters and sub-clusters. These four descriptors are the other angiosperms, the spores, the bisaccate pollen, and the dinoflagellate genus *Homotryblium*. The controlling percentage for all descriptors in each cluster and sub-cluster is presented on Fig. 8. Percentage time series for the 4 dominant descriptors are plotted in Figure 9 with 95% confidence intervals for the estimated percentages. This Percentage time series illustrates how the palynomorph groups are varying within statistically-defined clusters or sub-clusters and between clusters or sub-clusters. These results, with the SIMPER analysis results, are especially useful for characterizing paleoenvironmental changes at Site U1435 and constrain the timing of these key changes.

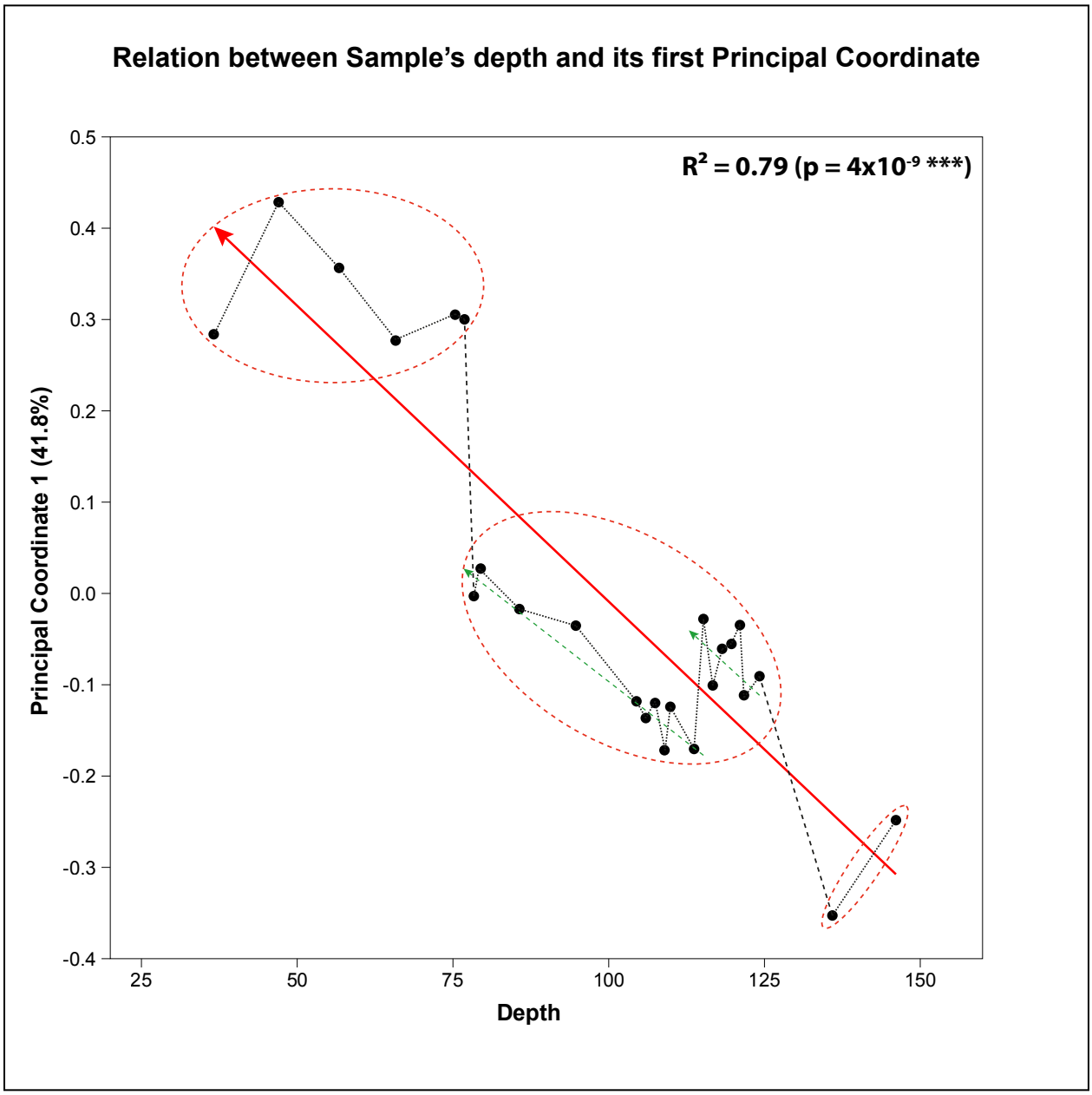

Figure 7. Principal Coordinates Analysis of the first Principal Coordinate against depth (PCo1 vs. Depth).

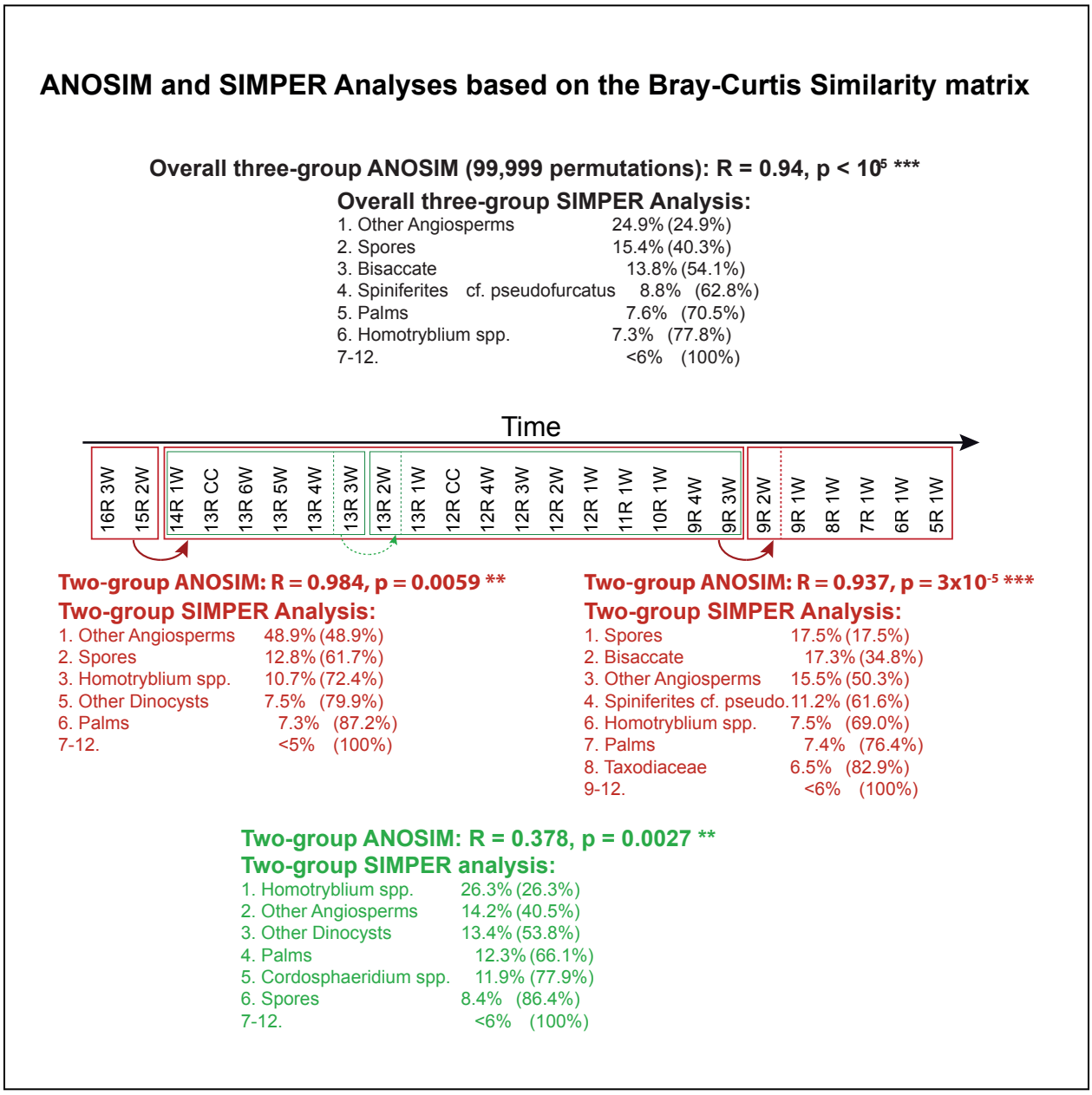

Figure 8. ANOSIM analyses showing variation between clusters from Figure 5 and SIMPER analyses describing the principal drivers of those variations.

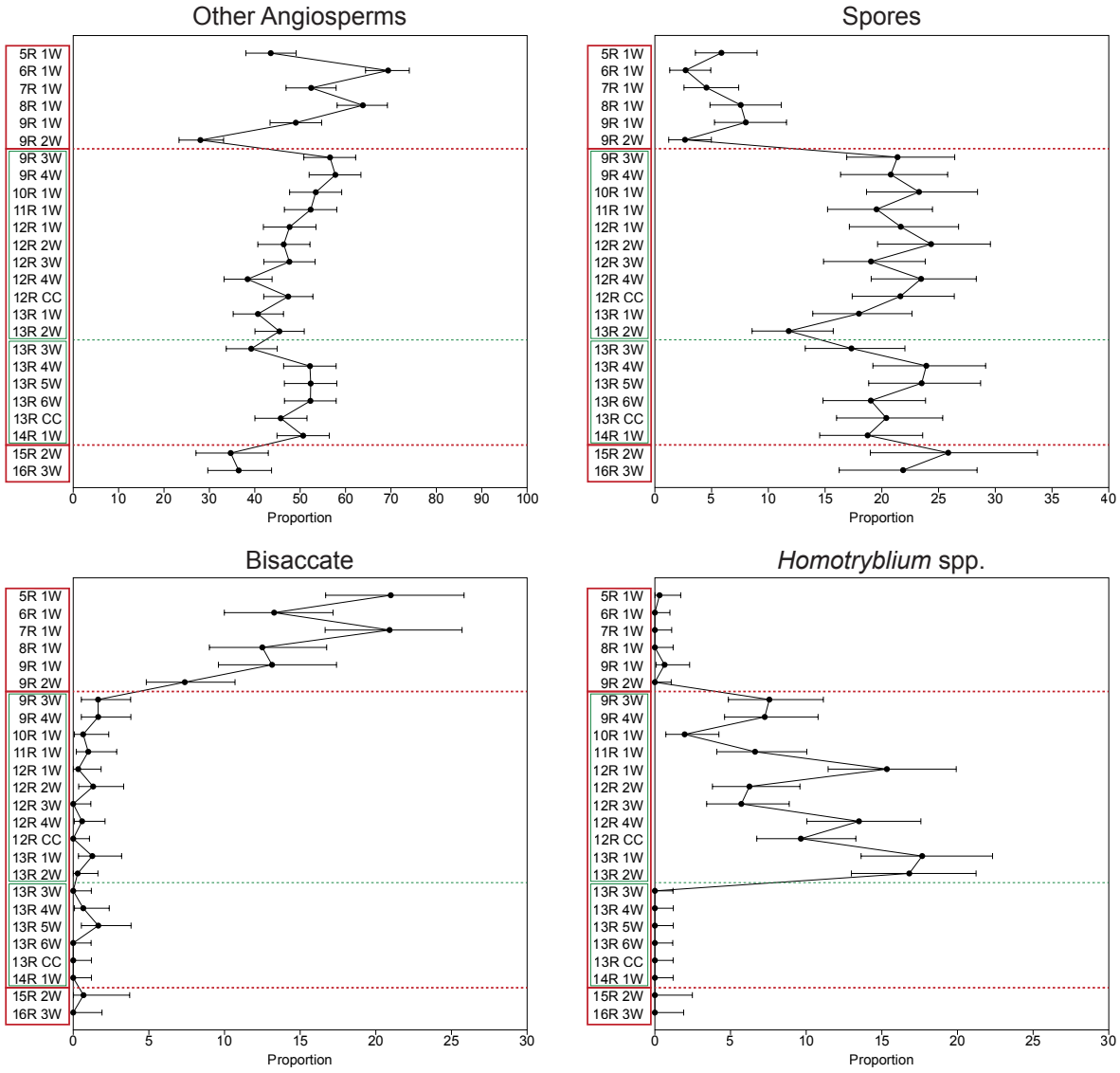

Figure 9. Percentage time series with 95% confidence intervals of 4 major descriptors (palynomorph groups) differentiating the clusters and sub-clusters from Figure 5.

4.2. Palynological zones

4.2.1. Zone 1

Zone 1 occurs from 298.50 mbsf to 153.26 mbsf, encompassing samples 17R 1W to 29R 1W of lithological Unit II and all samples of lithological Unit III (Fig. 4). This zone is characterized by very low to barren palynomorph recovery. Abundant black organic debris is observed within this zone, and the observed terrestrial and marine palynomorphs are much darker, ranging from brown to black, than those of the overlying zones. Statistically significant (>100) palynomorph recovery is not achieved within this zone, and thus no statistical analyses were performed on these samples.

4.2.2. Zone 2

Zone 2 occurs from 146.10 mbsf to 135.90 mbsf, encompassing samples 15R 2W and 16R 3W of lithological Unit II and corresponds to the first red box in Figure 5. Average concentration within this zone is 584 palynomorphs per gram of sediment. Terrestrial palynomorphs dominate with an average of 86.88% of the total palynomorph abundance. The "Other Angiosperms" group is most abundant within this zone (average 35.58%), while spores (average 23.86%) and palms (21.28%) are also abundant. *Spinizonocolpites* spp. is also consistently present within this zone (5.93%). Marine palynomorphs represent an average of only 13.12% of the assemblage, and are mostly marked by minor occurrences of species such as the dinoflagellate cyst *Lingulodinium machaerophorum* and the acritarch *Cyclopsiella* spp.

4.2.3 Zone 3

Zone 3 occurs from 124.20 mbsf to 78.35 mbsf, comprising samples 9R 3W to 14R 1W within lithological Unit II and corresponds to the second red box in Figure 5. Total concentrations within this zone range from 254 to 3383 palynomorphs per gram of sediment

(average of 1170 gdw^{-1}). Again, terrestrial palynomorphs dominate the assemblage (average 84.53%), primarily the "Other Angiosperms" group (a group including a variety of tropical flowering plants) with 38.42 to 57.76% (average of 48.59%). Bisaccate gymnosperms are rare in this assemblage, ranging from 0 to 1.66% (average of <1%). Taxodiaceae and Gramineae are also extremely rare, each averaging less than 1% (0 to 2.65% and 0 to 3.49%, respectively). Spores are much more abundant in this zone, ranging from 11.8 to 24.34% (average of 20.46%). Palms and *Spinizonocolpites* spp. are less prominent in this interval at 2.64 to 17.11% (average of 8.09%) and 1.32 to 8.97% (average of 5.08%), respectively.

The marine signal ranges from 6.29 to 31.37% (average of 15.47%) in this zone. The dinoflagellate cysts in this assemblage can be arranged into three prominent groups: *Spiniferites* spp., *Homotryblium* spp., and *Cordosphaeridium* spp., along with sporadic occurrences of other cysts. *Homotryblium* spp. is the dominant form, ranging from 0 to 82.14% (average of 39.18%). *Cordosphaeridium* spp. is also abundant in some samples, ranging from 0 to 68.75% (average of 14.45%). *Spiniferites* spp. ranges from 0 to 11.9% (average of 3.5%) of the marine signal in this zone.

Statistical analyses indicate that Zone 3 can be subdivided into two sub-zones (Figs. 4 & 5), described here as Zone 3A and Zone 3B. Zone 3A occurs from 124.20 mbsf to 116.70 mbsf (samples 13R 3W to 14R 1W) and corresponds to the first green box in Figure 5. Average concentration for Zone 3A is 652 palynomorphs per gram of sediment, and the "Other Angiosperms" group dominates with an average of 48.72%. Spores remain abundant with an average of 20.49%, followed by palms with an average of 9.64%. The mangrove *Spinizonocolpites* spp. remains consistently present with an average of 5.32%, and overall terrestrial palynomorphs constitute an average of 85.43%. Marine palynomorphs make up, on

average, the other 14.57% of the assemblage. Zone 3A is characterized by relatively abundant presence of *Cordosphaeridium* spp. (average 27.97% of marine signal) and minor *Spiniferites* spp. (average 2.70% of marine signal).

Zone 3B occurs from 115.20 mbsf to 78.35 mbsf (samples 9R 3W to 13R 2W) and corresponds to the second green box in Figure 5. Average concentration within this zone increases to 1452 palynomorphs per gram of sediment, but is still dominated by terrestrial palynomorphs (average 84.04%), mainly the "Other Angiosperms" group (average 48.52%). Spores still remain abundant (average 20.45%), but palms have slightly decreased to an average of 7.25%. *Spinizonocolpites* spp. remains relatively stable (average 4.94%), and Taxodiaceae increases from <1% to an average of 1.12%.

But of upmost interest, despite the dominance of terrestrial palynomorphs, Zone 3B is characterized by a clear increase in the marine signal (average 15.96%) with an acme in *Homotryblium* species. During that time interval, this genus averages 60.54% of the marine palynomorphs recovered, following its first occurrence at 115.20 mbsf in sample 13R 2W. *Cordosphaeridium* spp. decreases (average 7.07% of marine signal), while *Spiniferites* spp. remains low (average 3.94% of marine signal), a trend that changes markedly with the two samples marking the boundary between Zone 3 and Zone 4 (see details below).

4.2.4. Zone 4

Zone 4 occurs from 76.85 mbsf to 36.60 mbsf, encompassing samples 5R 1W to 9R 2W of lithological Unit IB and corresponds to the third red box in Figure 5. Average concentration again increases to an average of 1675 palynomorphs per gram of sediment in this zone. Terrestrial palynomorphs seems to have decreased slightly (average 80.49%), but this value is skewed by samples 9R 1W and 9R 2W that have much higher marine signals (average 42.31%)

than the other 4 samples in this zone (average 8.11%). Zone 4 differs markedly from the underlying Zones 1 to 3, notably by the dramatic increase in bisaccate pollen (average <1% Zones 1-3; average 14.70% Zone 4) and decrease in spores (average 5.23%). The "Other Angiosperms" group remains the major component (average 51.03%) of the terrestrial palynomorph assemblage, but palms (average 1.74%) and *Spinizonocolpites* spp. (average <1%) have decreased noticeably. Taxodiaceae increases to an average of 6.02% and Gramineae slightly increases to an average of 1.46%.

The marine signal in Zone 4 is skewed by the assemblages of samples 9R 1W and 9R 2W. For the entire zone, marine palynomorphs average 19.51%, but this value results from an average of 42.31% in samples 9R 1W and 9R 2W compared to an average of 8.11% for the other 4 samples. This is due to a sudden appearance and acme of a previously undescribed dinoflagellate cyst that appears only in these two samples, and is especially abundant in sample 9R 2W, with relative abundance increasing to 69.15% of the marine signal and a total concentration of 1039 cysts per gram of sediment. This species has a spherical central body with a smooth surface. Processes are smooth and hollow with wide, petaloid trifurcations; however, some appear "*ramosus* like." No intergonal processes are observed. Sutural septa are well expressed but low. The species resembles *Spiniferites pseudofurcatus*, but has a dissimilar wall structure and can have "*ramosus*-type" processes, so it is here described as *Spiniferites* cf. *pseudofurcatus* (see Plate 2). Note that because of the importance of this acme and its strategic position at the border between two lithological units and palynological zones, this species was reviewed and discussed in detail with Neogene dinoflagellate colleagues Dr. Laurent Londeix from the Universite de Bordeaux, Dr. Kenneth Mertens from Ifremer, and Dr. Stephen Louwye

at the University of Ghent (Belgium). All confirmed that this species is yet undescribed. Further work will be performed to formally describe this species.

Aside from the sudden appearance of *S.* cf. *pseudofurcatus*, other dinoflagellate species are less common, this include the *Homotryblium* spp. (average <1%) and *Cordosphaeridium* spp. (average 2.92%) signals that decrease dramatically in Zone 4. Other *Spiniferites* spp. (mostly *S. ramosus*-type) increase to an average of 14.05% but the overall marine signal from 65.80 mbsf to 36.60 mbsf (samples 5R 1W to 8R 1W) notably decreases and is less diverse; however, rare *Impagidinium* spp. first occur at 65.80 mbsf (sample 8R 1W) and remain present in small relative abundance to the top of the zone.

5. AGE ASSESSMENT

Within the dinoflagellate cyst assemblage, some stratigraphically significant species were identified (Fig. 10) and allow us to refine the age of Unit II of IODP Site U1435. This unit was previously ascribed a broad age of likely pre-Oligocene (Li et al. 2015) because of limitations associated to the poor recovery in calcareous-walled microfossil markers such as nannofossils and foraminifers. Age discussed herein are based on Damassa et al. (1994). *Cordosphaeridium fibrospinosum* is found in low abundances within Zone 3, but has a peak abundance at the top of Zone 3A at 116.70 mbsf (sample 13R 3W). Other *Cordosphaeridium* spp. (including *C. gracile* and *C. cantharellum*) are found in low abundances throughout Zone 3 and into the lower Zone 4 (75.35 mbsf to 76.85 mbsf, samples 9R 3W and 9R 1W). *Homotryblium plectilum* is the dominant form of the *Homotryblium* spp. identified in Zone 3B. *H. plectilum* first appears at 115.20 mbsf (sample 13R 2W) and is present throughout Zone 3B ranging from 14.29% to 82.14% (average 60.54%) of the marine signal. Other *Homotryblium* spp. (including *H. tenuispinosum*) are found within Zone 3B and appear rarely in Zone 4. Other dinoflagellate cyst species are only found sporadically and in very low concentrations but help constrain the likely age range of Zone 2 and Zone 3. These species include *Lingulodinium machaerophorum* and *Polysphaeridium zoharyi*.

Cordosphaeridium gracile and *C. fibrospinosum* both have FADs in the Late Cretaceous. *C. gracile* ranges into the Late Eocene (LAD: 36.0 Ma), while *C. fibrospinosum* has a more restricted range into the Middle Eocene (LAD: 47.5 Ma). *Cordosphaeridium cantharellum* also appears at Site U1435, but it is a younger species ranging from the Middle Eocene into the Early Miocene (41.0-22.0 Ma). *Homotryblium* is another useful species in the Eocene, with *H. tenuispinosum* (52.3-23.5 Ma) and *H. plectilum* (40.6-16.2 Ma) both observed at this site. Extant

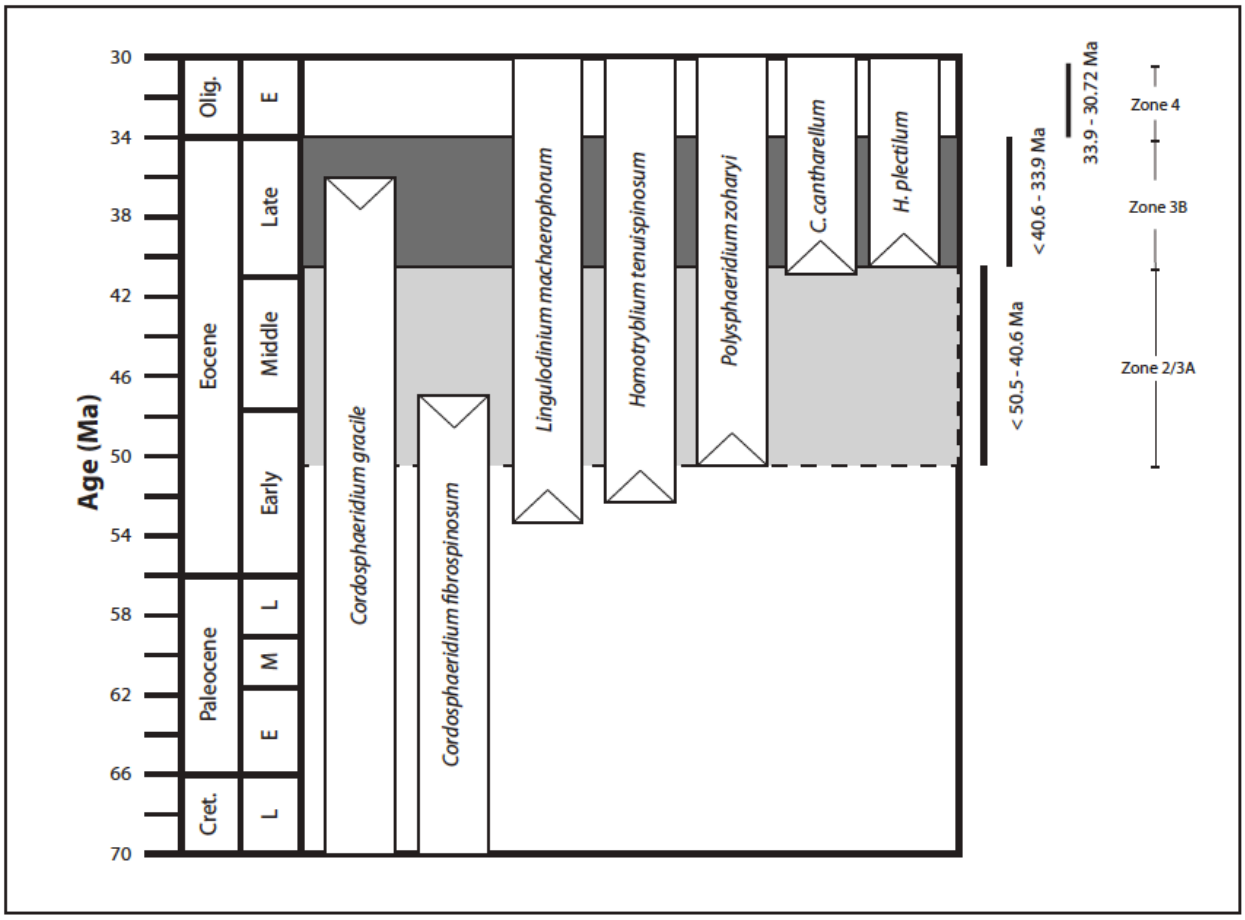

Figure 10. Age ranges of selected key dinoflagellate species used for age determination (Damassa et al. 1994) of Site U1435. Light grey shading indicates the proposed age range for Zone 2 and Zone 3A. Dark grey shading indicates proposed age of Zone 3B. Zone 4 age range base on Li et al. (2016). *C. cantharellum* = *Cordosphaeridium cantharellum*. *H. plectilum* = *Homotryblium plectilum.*

dinoflagellates that first appear in the Eocene are also useful for age constraints, especially *Lingulodinium machaerophorum* (53.5 Ma to present) and *Polysphaeridium zoharyi* (50.5 Ma to present) appearing throughout the cored section.

The first appearance datum (FAD) of *H. plectilum* is assigned to 40.6 Ma and is associated with the maximum flooding surface (mfs) within the TA3.5 sequence cycle at the Lutetian/Bartonian boundary (Haq et al. 1987). The first occurrence (FO) of *H. plectilum* at 115.20 mbsf corresponds with a marked decrease in the spores, bisaccates, and other angiosperms groups. A decrease in spore recovery is likely linked to rising sea levels (Poumot 1989), which is here interpreted as the TA3.5 mfs. Also noted is the presence of *L. machaerophorum* and *P. zoharyi* in the lowermost samples of Zone 2. Based on these marker species, Zone 2 and Zone 3 are assigned an age no older than the early to late Eocene. Zone 2 and 3A are determined to be between 50.5 – 40.6 Ma (Ypresian – Bartonian). The overlying Zone 3B is assigned an age of 40.6 to 33.9 Ma based on the FO of *H. plectilum* (Bartonian – Priabonian).

6. PALEOENVIRONMENTAL RECONSTRUCTION FROM THE RECOVERED PALYNOLOGICAL RECORD

Zone 1 is essentially barren of identifiable terrestrial or marine palynomorphs, but contains abundant brown to black organic matter. One explanation for this absence of palynomorphs could be conditions that prevented the deposition or preservation of palynomorphs at Site U1435 during this time. Palynomorph recovery is difficult in sand units (Gerneraad et al. 1968) like that of this zone; however, this explanation is unlikely, due to the recovery of palynomorphs in the lithologically similar units of Zone 2 and Zone 3. Another explanation is that barren samples are sometimes the result of thermal influence on the sediments caused by deep burial or tectonic influences, such as volcanism or proximity to intrusions (Germeraad et al. 1968; Correia 1970; Yule et al. 1998; Warny and Askin 2011a, 2011b). This explanation may be the most likely considering the tectonic complexity of the region, but further analysis is necessary to confirm. If igneous intrusions are indeed the cause of the low recovery in the lower part of Site U1435, then these intrusions would have lowered in intensity at the base of the first stastistically valid zone (sample 16 R3), possibly in the early to middle Eocene based on our biostratigraphic zonation (Fig. 10).

The palynological samples of Zone 2 to Zone 4 are characterized here by the variations of 12 environmentally or stratigraphically significant palynomorph groups. The terrestrial palynomorph groups are based on those presented by Poumot (1989) for identifying eustatic events in tropical settings. All spores are grouped together and interpreted as more abundant in areas with increased fluvial activity (Poumot 1989). Taxodiaceae (and fossil forms) are grouped and are indicative of swamp settings (Farley 1990). Bisaccate gymnosperms are grouped together and are known to become more abundant during periods of cooling, indicating the

extension of the temperate zone (Poumot 1989). However, bisaccate pollen are more easily transported in greater distances; therefore, increases in relative abundance may represent a more distal relationship to the shore (Sun et al. 2000; Warny et al. 2003). In the absence of other herbaceous taxa, such as Compositae and Amaranthaceae-Chenopodiaceae, the group including all Gramineae is the only representative of the herb signal at Site U1435, but it also may indicate falling sea level (Germeraad et al. 1968; Poumot 1989). Palm taxa are grouped together (mostly monocolpate/monosulcate grains and *Dicolpopollis* spp.) and likely occupied a sandy coastline setting (Poumot 1989). The fossil form of *Nypa*, *Spinizonocolpites* spp., is known to be the principal mangrove species in the Eocene of Southeast Asia (Germeraad et al. 1968; Muller et al. 1968; Morley 1977; Thanikaimoni 1987) and it is indeed the major component of our mangrove assemblage (thus providing an additional support for our proposed age assignment). All other angiosperm pollens are grouped together, mostly comprising a very diverse assemblage of sub-tropical to tropical flowering plants.

For the marine palynomorph groups, the three dominant genera at Site U1435 are *Cordosphaeridium* spp., *Homotryblium* spp., and *Spiniferites* spp. The form *S.* cf. *pseudofurcatus* is treated as a group separate from *Spiniferites* spp. due to its unique appearance and acme in the two lowermost Zone 4 samples. No other dinoflagellate cyst genera are consistently or significantly present at Site U1435, so any other dinoflagellate cysts and acritarchs are grouped together. *Cordosphaeridium* taxa were likely deposited within open sea environments (Islam 1984; Mudie and Harland 1996; Jaramillo and Oboh-Ikuenobe 1999). Previous studies have shown that *Homotryblium* taxa likely inhabited marginal marine to restricted marine or lagoonal, hypersaline settings (Brinkhuis 1994; Zevenboom et al. 1994; Dale 1996). Others have suggested that *Homotryblium* taxa were also capable of surviving in low-salinity environments (Dybkjær

2004). The species of the genus *Homotryblium* also likely favored warmer waters (Williams and Bujak 1977) and can occur as the dominant component in low diversity assemblages, including unstable coastal environments (de Verteuil and Norris 1996; Pross and Schmiedl 2002). Extensive studies have examined the genus *Spiniferites* spp., and determined them to be overall indicative of a variety of environments from neritic to open marine conditions (Downie et al. 1971; Wall et al. 1977; Harland 1983; Islam 1984; Brinkhuis 1994; Warny and Wrenn 1997).

Zone 2 and Zone 3 have been assigned here to middle to late Eocene in age based on dinoflagellate species appearances (Fig. 10). The differences in both terrestrial and marine palynomorph assemblages between Zone 2 and Zone 3 are slight and not easily discernible. As shown in the ANOSIM and SIMPER analyses (Fig. 8), the "Other Angiosperms" group and spores account for most of the dissimilarity between the two zones. "Other Angiosperms" increases from Zone 2 to Zone 3, but spores decrease slightly between the two zones. Overall, Zone 2 and Zone 3 assemblages suggest a relatively stable, warm and everwet environment throughout the Middle and Late Eocene at Site U1435 (Germeraad et al. 1968; Thanikaimoni 1987; Poumot 1989). Zone 2 and Zone 3 were likely deposited in a fluvial or nearshore setting as indicated by the consistent presence of the mangrove *Spinizonocolpites* spp. (Muller 1968; Morley RJ and Morley HP 2013), the abundant spore assemblage and low bisaccate relative abundance (Poumot1989) and the dinoflagellate assemblage, dominated by *Homotryblium* spp. (Dybkjær 2004; Sluijs et al. 2005). These results are in agreement with the shipboard descriptions of lithological Unit II and analysis of benthic foraminifers (Expedition 349 Scientists 2014).

Within Zone 3, Zones 3A and 3B differ based on the dinoflagellate assemblage and also the "Other Angiosperms" group. The obvious change from Zone 3A to Zone 3B is the first

appearance and acme in *Homotryblium* spp. throughout Zone 3B until the Zone 3/Zone 4 boundary. A decrease in spores and other palynomorphs in the lowermost sample of Zone 3B is noteworthy. As mentioned above, this event is proposed to be associated with the TA3.5 sequence cycle maximum flooding surface. This event and the appearance of *Homotryblium* spp., dominated by *H. plectilum*, are the key discernible changes across these two sub-zones.

Both the terrestrial and marine palynomorph assemblages show two markedly different environments across the breakup unconformity marking what is thought to be the initiation of seafloor spreading at Site U1435 (Li et al. 2015). The ANOSIM and SIMPER analyses (Fig. 8) illustrate that the middle to late Eocene terrestrial assemblage of Zone 2 and Zone 3 differ from that of early Oligocene Zone 4 largely on changes in spores, bisaccate pollen, and the "Other Angiosperms" group across the breakup unconformity. The dramatic decrease in spores concurrent with the increase in bisaccate pollen and the "Other Angiosperms" group could be indicative of early Oligocene cooling (Zachos et al. 2001) or a decreased fluvial input and deeper regime following the initiation of seafloor spreading (Mao et al. 2007; Luo et al. 2014). A noticeable decrease in palms and *Spinizonocolpites* spp. also occurs across this boundary between Zone 3 and Zone 4.

The first appearance and acme of *Spiniferites* cf. *pseudofurcatus* at the bottom of Zone 4 also marks a change across the Zone 3/Zone 4 boundary. *Spiniferites* spp. are found today in mostly higher salinity, open marine environments (Zonneveld et al. 2013). The appearance of this genus is in agreement with the results of foraminifer studies on this section suggesting outer-shelf to slope settings (Li at al. 2016); however, its sudden disappearance and the overall low concentration and diversity of the dinoflagellate assemblage above 75.35 mbsf (sample 9R 1W) is unexpected.

7. CONCLUSIONS

Analysis of organic-walled microfossils indicates a likely Ypresian – Priabonian age for the sediments underlying the South China Sea breakup unconformity at IODP Site U1435. The first occurrence of *Homotryblium plectilum* corresponds with a rise in sea level that is interpreted here as the TA3.5 maximum flooding surface at 41.2 Ma (Haq et al. 1987). In addition to critical age control, this study provides insight into rarely observed Eocene deposits in the South China Sea. Site U1435 experienced stable, warm everwet conditions in a nearshore, likely fluvial or deltaic setting throughout the middle to late Eocene. The Eocene Oligocene boundary is marked by an acme in a new dinoflagellate spcies; *Spiniferites* cf. *pseudofurcatus*; which is described for the first time herein. The early Oligocene climate sampled at IODP Site U1435 remains warm, but it noticeably cooler than the underlying Eocene section sampled as evidenced by a marked increase in conifer trees (bissacate pollen) and the decrease in tropical species such as palm, mangroves and ferns.

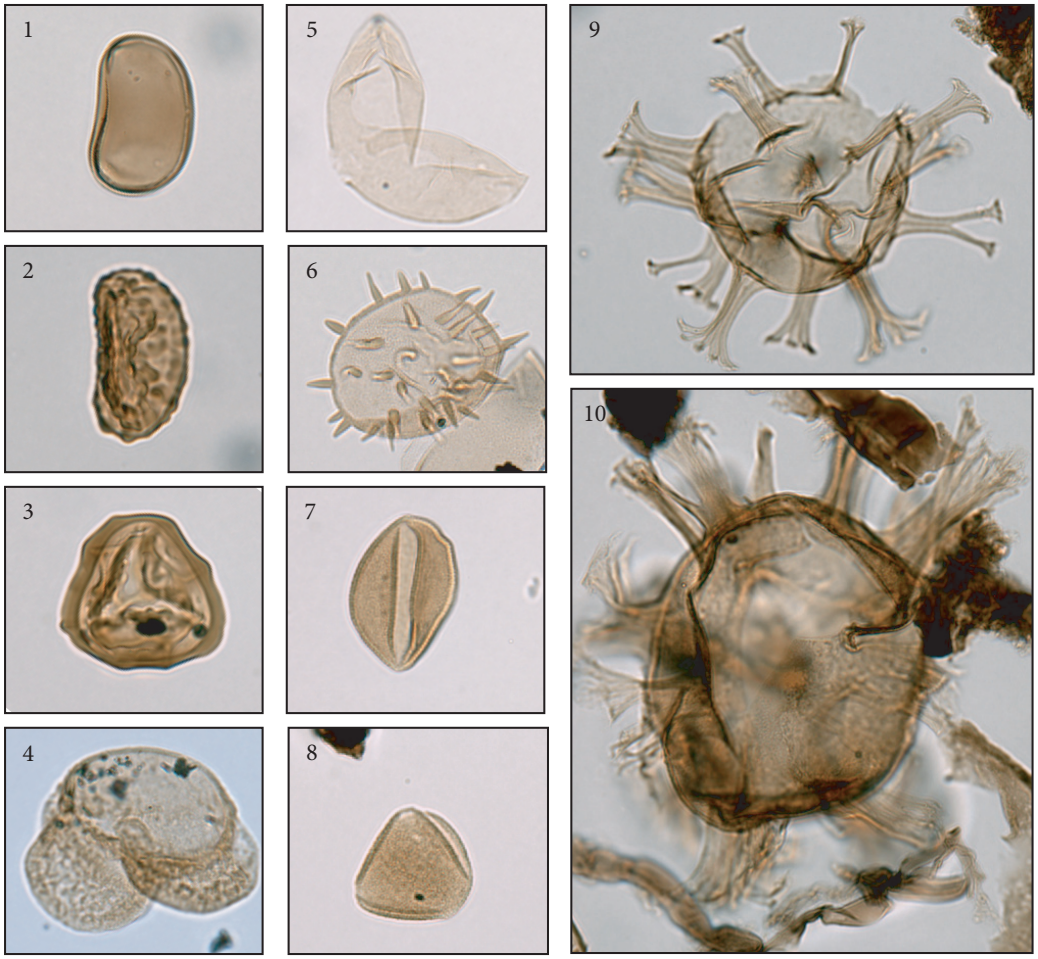

Plate 1. Light photomicrographs of terrestrial and marine palynomorphs from IODP Site U1435. (All specimens are imaged at 600x magnification.) 1. *Polypodiaceaesporites* sp., 12R 4W (108.95 m). 2. *Polypodiisporites* sp., 13R 4W (118.20 m). 3. *Polypodiaceoisporites* sp., 12R 2W (105.95 m). 4. Pinaceae, 5R 1W (36.60 m). 5. Taxodiaceae, 7R 1W (56.72 m). 6. *Spinizonocolpites* sp., 12R CC (109.89 m). 7. Arecaceae (palm), 14R 1W (124.20 m). 8. *Dicolpopollis* sp., 13R 6W (121.06 m). 9. *Homotryblium plectilum*, 13R 2W (115.20 m). 10. *Cordosphaeridium fibrospinosum*, 13R 3W (116.70 m).

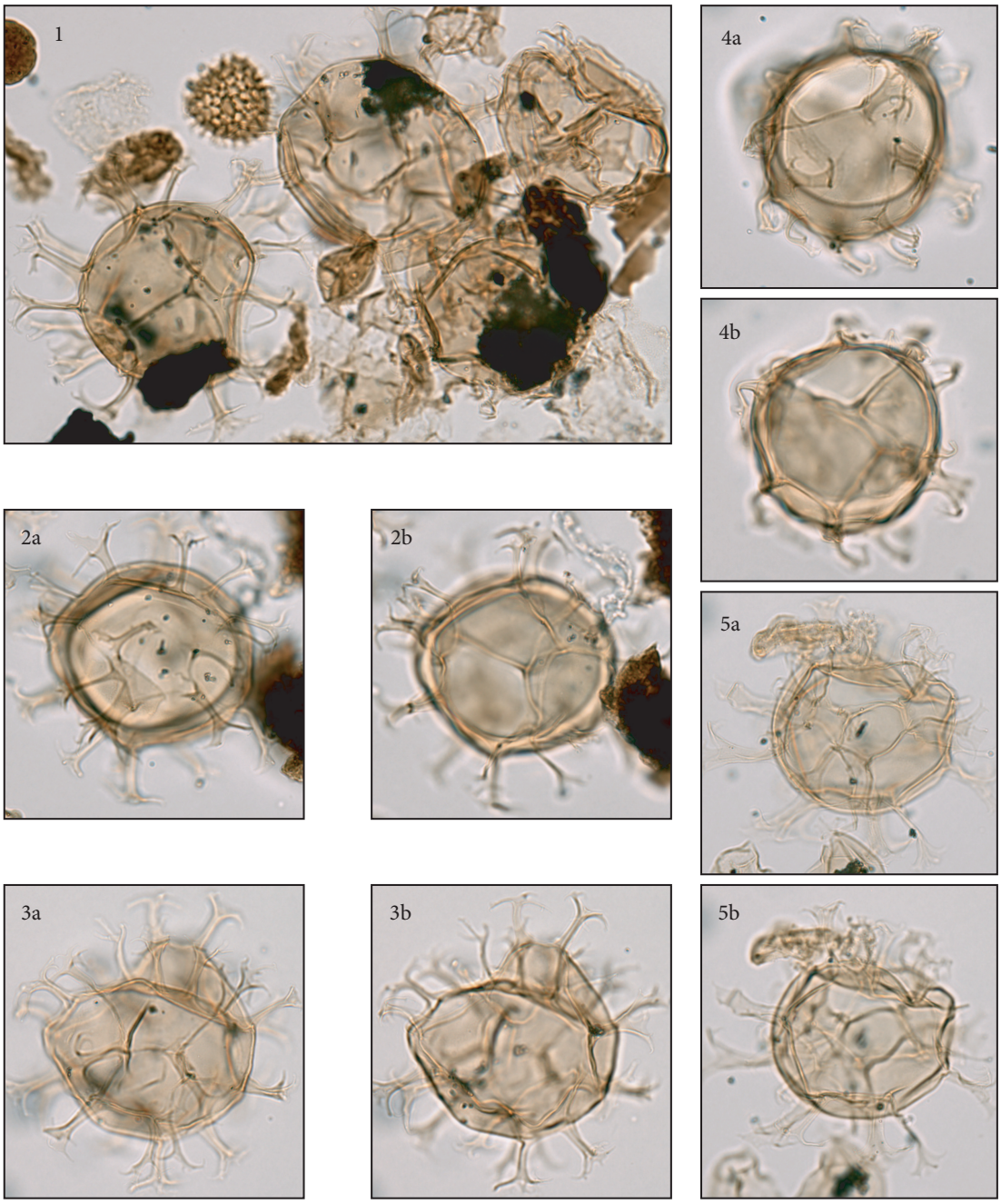

Plate 2. 1-5. Light photomicrographs of *Spiniferites* cf. *pseudofurcatus* specimens from samples 9R 1W and 9R 2W. 1, 4, 5. 9R 1W (75.35 m). 2, 3. 9R 2W (76.85 m).

REFERENCES

Benninghoff WS. 1962. Calculation of pollen and spores density in sediments by addition of exotic pollen in known quantities. *Pollen et Spores* 6, 332–333.

Briais A, Patriat P, Tapponnier P. 1993. Updated interpretation of magnetic anomalies and seafloor spreading stages in the South China Sea: implications for the Tertiary tectonics of Southeast Asia. *Journal of Geophysical Research: Solid Earth* 98(B4), 6299–6328.

Brinkhuis H. 1994. Late Eocene to Early Oligocene dinoflagellate cysts from the Priabonian type-area (Northeast Italy): biostratigraphy and paleoenvironmental interpretation. *Palaeogeography, Palaeoclimatology, Palaeoecology* 107(1), 121-163.

Brown CA. 2008. *Palynological Techniques*, 2nd ed.. Riding JB, Warny S. (eds). American Association of Stratigraphic Palynologists.

Correia M. 1970. Diagenesis of sporopollenin and other comparable organic substances: application to hydrocarbon research. Symposium On Sporopollenin.

Dale B. 1996. Dinoflagellate cyst ecology: modeling and geological applications. *Palynology: principles and applications* 1249-1275.

Damassa SP, Williams GL, Brinkhuis,H, Bujak JP, Powell J. 1994. Short course in Paleogene dinoflagellate cysts. Utrecht.

de Verteuil L, Norris G. 1996. Middle to upper Miocene Geonettia clineae, an opportunistic coastal embayment dinoflagellate of the Homotryblium Complex. *Micropaleontology* 263-284.

Downie C, Hussain MA, Williams GL. 1971. Dinoflagellate cyst and acritarch associations in the Paleogene of southeast England. *Geoscience and Man* 3(1), 29-35.

Dybkjær K. 2004. Morphological and abundance variations in Homotryblium-cyst assemblages related to depositional environments; uppermost Oligocene–Lower Miocene, Jylland, Denmark. *Palaeogeography, Palaeoclimatology, Palaeoecology* 206(1), 41-58.

Expedition 349 Scientists. 2014. South China Sea tectonics: opening of the South China Sea and its implications for southeast Asian tectonics, climates, and deep mantle processes since the late Mesozoic. International Ocean Discovery Program Preliminary Report, 349.

Farley MB. 1990. Vegetation distribution across the early Eocene depositional landscape from palynological analysis. *Palaeogeography, Palaeoclimatology, Palaeoecology* 79(1-2), 11-27.

Flower MFJ, Russo RM, Tamaki K, Hoang N. 2001. Mantle contamination and the Izu-Bonin-Mariana (IBM) "high-tide mark": evidence for mantle extrusion caused by Tethyan closure. *Tectonophysics* 333(1–2), 9–34.

Germeraad JH, Hopping CA, Muller J. 1968. Palynology of Tertiary sediments from tropical areas. *Review of palaeobotany and palynology* 6(3-4), 189200212230261263-198210228259348.

Hall R. 2002. Cenozoic geological and plate tectonic evolution of SE Asia and the SW Pacific: computer-based reconstructions, model and animations. *Journal of Asian Earth Sciences* 20(4), 353–431.

Harland R. 1983. Distribution maps of recent dinoflagellate cysts in bottom sediments from the North-Atlantic Ocean and adjacent seas. *Palaeontology* 26(May), 321-387.

Holloway NH. 1982. North Palawan Block, Philippines: its relation to the Asian mainland and role in evolution of South China Sea. AAPG Bulletin 66(9), 1355–1383.

Islam MA. 1984. A study of Early Eocene palaeoenvironments in the Isle of Sheppey as determined from microplankton assemblage composition. *Tertiary Research* 6(1), 11-21.

Jahn BM, Chen PY, Yen TP. 1976. Rb-Sr ages of granitic rocks in southeastern China and their tectonic significance. Geological Society of America Bulletin 87(5), 763–776.

Jaramillo CA Oboh-Ikuenobe FE. 1999. Sequence stratigraphic interpretations from palynofacies, dinocyst and lithological data of Upper Eocene–Lower Oligocene strata in southern Mississippi and Alabama, US Gulf Coast. *Palaeogeography, Palaeoclimatology, Palaeoecology* 145(4), 259-302.

Leloup PH, Arnaud N, Lacassin R, Kienast JR, Harrison TM, Trong TTP, Replumaz A, Tapponnier P. 2001. New constraints on the structure, thermochronology, and timing of the Ailao Shan-Red River shear zone, SE Asia. *Journal of Geophysical Research: Solid Earth* 106(B4), 6683–6732.

Li C, Xu X, Lin J, Sun Z, Zhu J, Yao Y, Zhao X, Liu Q, Kulhanek DK, Wang J. 2014. Ages and magnetic structures of the South China Sea constrained by deep tow magnetic surveys and IODP Expedition 349. *Geochemistry, Geophysics, Geosystems* 15, 4958–4983, doi:10.1002/2014GC005567.

Li C, Lin J, Kulhanek D, the Expedition 349 Scientists. 2015. Site U1433. Proceedings of the International Ocean Discovery Program, 349, doi:10.14379/iodp.proc.349.105.2015

Li Q, Cheng X, Chen J, Xu J. 2016. Data report: Oligocene foraminifers and stable isotopes from IODP Hole U1435A. In Li CF, Lin J, Kulhanek DK, the Expedition 349 Scientists. South China Sea Tectonics. Proceedings of the International Ocean Discovery Program, 349:

College Station, TX (International Ocean Discovery Program). http://dx.doi.org/10.14379/iodp.proc.349.201.2016

Luo C, Chen M, Xiang R, Liu J, Zhang L, Lu J, Yang M. 2014. Modern pollen distribution in marine sediments from the northern part of the South China Sea. *Marine Micropaleontology* 108, 41-56.

Mao S, Li J, Qin X, Wu G, Harland R. 2007. Dinoflagellate cysts and environmental evolution of the Oligocene to Lower Miocene at site 1148, Odp Leg 184, South China Sea. *Palynology* 31(1), 37-52.

Morley RJ. 1977. Palynology of Tertiary and Quaternary sediments in southeast Asia.

Morley RJ,, Morley HP. 2013. Mid Cenozoic freshwater wetlands of the Sunda region. *Journal of Limnology* 72(s2), 2.

Mudie PJ, Harland R. 1996. Aquatic quaternary. *Palynology: principles and applications* 2, 843-877.

Muller J. 1968. Palynology of the Pedawan and plateau sandstone formations (Cretaceous-Eocene) in Sarawak, Malaysia. *Micropaleontology* 1-37.

Poumot C. 1989. Palynological evidence for eustatic events in the tropical Neogene. Bulletin des Centres de Recherches Exploration-Production Elf Aquitaine 13(2), 437-453.

Pross J, Schmiedl G. 2002. Early Oligocene dinoflagellate cysts from the Upper Rhine Graben (SW Germany): paleoenvironmental and paleoclimatic implications. *Marine Micropaleontology* 45(1), 1-24.

Sluijs A, Pross J, Brinkhuis H. 2005. From greenhouse to icehouse; organic-walled dinoflagellate cysts as paleoenvironmental indicators in the Paleogene. *Earth-Science Reviews* 68(3), 281-315.

Sun X, Li X, Luo Y, Chen X. 2000. The vegetation and climate at the last glaciation on the emerged continental shelf of the South China Sea. *Palaeogeography, Palaeoclimatology, Palaeoecology* 160(3), 301-316.

Tapponnier P, Peltzer G, Le Dain AY, Armijo R, Cobbold P. 1982. Propagating extrusion tectonics in Asia: new insights from simple experiments with plasticene. *Geology* 10(12):611–616.

Taylor B, Hayes DE. 1980. The tectonic evolution of the South China Basin. In Hayes DE. (ed), The Tectonic and Geologic Evolution of Southeast Asian Seas and Islands. *Geophysical Monograph* 23, 89–104.

Taylor B, Hayes DE. 1983. Origin and history of the South China Sea Basin. In Hayes DE. (ed), The Tectonic and Geologic Evolution of Southeast Asian Seas and Islands (Pt. 2). *Geophysical Monograph* 27, 23–56.

Thanikaimoni G. 1987. Mangrove palynology. *Travaux de la Section Scientifique et Technique, Institut Français de Pondichéry* 24, 1-100.

Wall D, Dale B, Lohmann, GP, Smith WK. 1977. The environmental and climatic distribution of dinoflagellate cysts in modern marine sediments from regions in the North and South Atlantic Oceans and adjacent seas. *Marine micropaleontology* 2, 121-200.

Warny S, Wrenn JH. 1997. New species of Dinoflagellate cysts from the Miocene-Pliocene boundary on the Atlantic coast of Morocco. *Paleaobotany and Palynology* 96, 281-304.

Warny S, Bart PJ, Suc JP. 2003. Timing and progression of climatic, tectonic and glacioeustatic influences on the Messinian Salinity Crisis. *Palaeogeography, Palaeoclimatology and Palaeoecology* 202(1-2), 59-66.

Warny S, Askin R. 2011b. Last remnants of Cenozoic vegetation and organic-walled phytoplankton in the Antarctic Peninsula's icehouse world. *AGU Special Publication* 63, 167-192. doi: 10.1029/2010SP000996.

Warny S, Askin R. 2011a. Vegetation and organic-walled phytoplankton at the end of the Antarctic greenhouse world: latest cooling events. *AGU Special Publication* 63, 193-210. doi: 10.1029/2010SP000965.

Williams GL, Bujak JP. 1977. Distribution patterns of some North Atlantic Cenozoic dinoflagellate cysts. *Marine Micropaleontology* 2, 223-233.

Xu Y, Wei J, Qiu H, Zhang H, Huang X. 2012. Opening and evolution of the South China Sea constrained by studies on volcanic rocks: preliminary results and a research design. Chinese Science Bulletin 57(24), 3150–3164.

Yule B, Roberts S, Marshall JEA, Milton JA. 1998. Quantitative spore colour measurement using colour image analysis. *Organic Geochemistry* 28(3), 139-149.

Zachos J, Pagani M, Sloan L, Thomas E, Billups K. 2001. Trends, rhythms, and aberrations in global climate 65 Ma to present. *Science* 292(5517), 686-693.

Zhou XM, Li WX. 2000. Origin of late Mesozoic igneous rocks in southeastern China: implications for lithosphere subduction and underplating of mafic magmas. *Tectonophysics* 326(3–4), 269–287.

Zevenboom D, Brinkhuis H, Visscher H. 1994. Dinoflagellate cysts palaeoenvironmental analysis of the Oligocene/Miocene transition in northwest and central Italy. *Giornale di Geologia* 56(1), 155-169.

Zonneveld KA, Marret F, Versteegh GJ, Bogus K, Bonnet S, Bouimetarhan I, Esper O. 2013. Atlas of modern dinoflagellate cyst distribution based on 2405 data points. *Review of Palaeobotany and Palynology* 191, 1-197.

APPENDIX. PALYNOLOGICAL COUNTS

Sample	Depth (mbsf)	Weight (g)	Lycopodium	Spores	Taxodiaceae	Bisaccate	Gramineae	Palms	*Spinizonocolpites* spp.	Other Angiosperms	*Cordosphaeridium* spp.	*Homotryblium* spp.	*Spiniferites* cf. *pseudofurcatus*	*Spiniferites* spp.	Other Dinocysts	Total
5R 1W	36.60	3.4	1536	19	38	68	7	14	1	141	-	1	-	9	26	324
6R 1W	47.02	3.4	794	10	26	49	15	3	-	256	-	-	-	1	9	369
7R 1W	56.72	5.5	795	15	34	69	2	6	1	173	-	-	-	6	24	330
8R 1W	65.80	2.7	2025	23	8	38	3	7	2	194	-	-	-	6	23	304
9R 1W	75.35	8.1	1255	25	11	41	3	-	-	153	4	2	42	6	25	312
9R 2W	76.85	8.2	340	9	3	25	-	4	2	95	25	-	139	2	35	339
9R 3W	78.35	4.1	457	65	6	5	-	16	4	172	3	23	-	2	8	304
9R 4W	79.45	4.6	444	63	8	5	2	8	6	175	-	22	-	1	13	303
10R 1W	85.66	5.0	900	71	1	2	-	14	12	163	4	6	-	5	27	305
11R 1W	94.72	5.6	992	59	4	3	9	13	20	158	2	20	-	3	11	302
12R 1W	104.45	5.6	487	65	1	1	2	15	17	143	1	46	-	-	9	300
12R 2W	105.95	7.1	946	74	2	4	3	28	25	141	2	19	-	-	6	304
12R 3W	107.45	8.7	1280	60	2	-	11	40	20	150	1	18	-	1	12	315
12R 4W	108.95	7.3	1144	80	1	2	1	32	19	131	8	46	-	4	17	341
12R CC	109.89	5.4	1064	74	2	-	2	35	15	162	12	33	-	-	7	342
13R 1W	113.70	11.5	761	57	3	4	3	37	14	129	3	56	-	3	8	317
13R 2W	115.20	15.9	1593	40	9	1	-	16	20	154	4	57	-	2	36	339
13R 3W	116.70	12.3	764	53	2	-	-	20	15	120	66	-	-	4	26	306
13R 4W	118.20	10.2	623	72	1	2	-	18	27	157	6	-	-	2	16	301
13R 5W	119.70	17.0	558	71	5	5	2	24	18	158	6	-	-	-	13	302
13R 6W	121.06	11.9	874	59	-	-	1	21	13	162	12	-	-	2	40	310

Sample	Depth (mbsf)	Weight (g)	Lycopodium	Spores	Taxodiaceae	Bisaccate	Gramineae	Palms	*Spinizonocolpites* spp.	Other Angiosperms	*Cordosphaeridium* spp.	*Homotryblium* spp.	*Spiniferites* cf. *pseudofurcatus*	*Spiniferites* spp.	Other Dinocysts	Total
13R CC	121.70	17.6	1415	62	2	-	1	41	10	139	6	-	-	-	43	304
14R 1W	124.20	7.5	1192	57	-	-	2	52	14	154	2	-	-	-	23	304
15R 2W	135.90	12.2	656	38	-	1	-	37	9	51	-	-	-	-	11	147
16R 3W	146.10	16.6	307	42	-	-	-	33	11	70	-	-	-	-	36	192
17R 1W	153.26	13.4	229	19	1	1	-	11	2	19	1	-	42	-	6	60
18R 2W	164.19	16.9	323	27	-	-	-	14	8	13	3	-	139	-	3	68
19R 1W	172.33	17.6	418	7	-	-	-	22	4	57	3	-	-	-	6	99
20R 1W	182.38	13.8	342	2	-	-	-	11	4	8	-	-	-	-	-	25
21R 1W	191.99	6.4	6033	2	-	2	-	6	2	3	-	-	-	-	-	15
23R 1W	210.98	16.4	493	2	-	-	-	3	2	5	-	-	-	-	-	12
23R 2W	212.47	22.9	257	-	-	-	-	3	3	-	-	-	-	-	-	6
23R 3W	213.97	11.3	907	-	-	-	-	-	1	3	-	-	-	-	-	4
23R 4W	215.60	20.9	290	-	-	-	-	-	-	-	-	-	-	-	-	-
23R 5W	217.01	12.9	879	-	-	-	-	3	-	5	-	-	-	-	-	8
23R CC	218.07	7.8	1623	-	-	-	-	-	-	2	-	-	-	-	-	2
24R 2W	222.80	21.4	424	-	-	-	-	-	-	-	-	-	-	-	-	-
24R 5W	227.13	19.9	249	-	-	-	-	-	-	-	-	-	-	-	-	-
25R 2W	231.90	20.4	337	-	-	-	-	-	4	4	-	-	-	-	-	8
26R 5W	246.81	10.5	730	4	-	-	-	-	5	2	-	-	-	-	-	11
27R 5W	255.98	20.3	181	-	-	-	-	-	-	-	-	-	-	-	-	-
28R 1W	260.12	9.4	211	-	-	-	-	-	2	-	-	-	-	-	-	2

Sample	Depth (mbsf)	Weight (g)	Lycopodium	Spores	Taxodiaceae	Bisaccate	Gramineae	Palms	*Spiniferites* spp.	Other Angiosperms	*Cordosphaeridium* spp.	*Homotryblium* spp.	*Spiniferites* cf. *pseudofurcatus*	*Spiniferites* spp.	Other Dinocysts	Total
29R 1W	269.10	20.3	381	-	-	-	-	-	-	-	-	-	-	-	-	-
30R 1W	279.10	11.5	2923	-	-	-	-	-	3	-	-	-	-	-	-	3
31R 1W	288.75	13.3	370	1	-	-	-	-	6	-	-	-	-	-	-	7
32R 1W	298.50	11.2	1096	-	-	-	-	-	-	-	-	-	-	-	-	-

VITA

Mitchell Gregory was born and raised in Baton Rouge, Louisiana. He graduated from Louisiana State University in 2014 with a B.S. in Geology and a minor in Business Administration. After completing his Master's, Mitchell intends to move to Houston to intern with PetroStrat Inc.